JAIST Repository
https://dspace.jaist.ac.jp/

Title	Fullerene-encapsulated porphyrin hexagonal nanorods. An anisotropic donor-acceptor composite for efficient photoinduced electron transfer and light energy conversion
Author(s)	Hasobe, Taku; Sandanayaka, Atula S. D.; Wada, Takehiko; Araki, Yasuyuki
Citation	Chemical Communications(29): 3372-3374
Issue Date	2008
Type	Journal Article
Text version	author
URL	http://hdl.handle.net/10119/8827
Rights	Copyright (C) 2008 Royal Society of Chemistry. Taku Hasobe, Atula S. D. Sandanayaka, Takehiko Wada and Yasuyuki Araki, Chemical Communications, (29), 2008, 3372-3374. http://dx.doi.org/10.1039/b806748a - Reproduced by permission of The Royal Society of Chemistry
Description	

JAIST
JAPAN
ADVANCED INSTITUTE OF
SCIENCE AND TECHNOLOGY

Japan Advanced Institute of Science and Technology

Fullerenes-encapsulated porphyrin hexagonal nanorods. An anisotropic donor-acceptor composite for efficient photoinduced electron transfer and light energy conversion

Taku Hasobe,*[ab] Atula S. D. Sandanayaka,*[a] Takehiko Wada[c] and Yasuyuki Araki[c]

Received (in XXX, XXX) 1st January 2007, Accepted 1st January 2007
First published on the web 1st January 2007
DOI: 10.1039/b000000x

We have successfully constructed fullerenes-encapsulated porphyrin hexagonal nanorods in DMF/acetonitrile solution mixed with surfactant, which demonstrate efficient and characteristic photoinduced electron transfer and light energy conversion properties.

Construction of functional molecular assemblies with well-defined shapes and structures are of great interest because of a variety of applications such as optoelectronics.[1] Porphyrins are major and promising building blocks for such organized nanoscale superstructures,[2] which perform many of the essential light-harvesting and photoinduced electron/energy transfer reactions.[3,4] Unidirectionally bar-shaped nanostructures of porphyrins (i.e. porphyrin nanorods and nanotubes) also have potentials for fabrication of nanoscale materials, electronics and photonics because of the characteristic anisotropic structures.[5] However, little attention has been given to utilize such structures in electronic and optical applications.[5b]

Fullerenes incidentally hold a great promise as a spherical electron acceptor on account of their small reorganization energy in electron transfer reactions.[3,6] Combination of both porphyrins and fullerenes seems ideal for fulfilling an enhanced light-harvesting efficiency of chromophores throughout the solar spectrum and a highly efficient conversion of the harvested light into the high energy state of the charge separation by photoinduced electron transfer (PET).[3,6]

Here we report a new type of molecular composites: fullerenes-encapsulated porphyrin hexagonal nanorods composed of zinc *meso*-tetra (4-pyridyl) porphyrin [$ZnP(Py)_4$] and C_{60} [denoted as C_{60}-$ZnP(Py)_4$ nanorod], which are prepared by aiding surfactant: cetyltrimethylammonium bromide (CTAB) in a DMF/acetonitrile mixed solvent (Fig. 1). The highly organized C_{60}-$ZnP(Py)_4$ nanorods demonstrate that not only a broad absorption property derived from the supramolecular aggregates, but also significant enhancement of solar energy conversion property based on photoinduced charge separation (CS) yielding radical ion pair [$C_{60}^{\bullet-}$–$ZnP(Py)_4^{\bullet+}$].

$ZnP(Py)_4$ (Aldrich) was purified by recrystallization before use. C_{60}-$ZnP(Py)_4$ nanorods were prepared as follows (Fig. 1).

[a]School of Materials Science, Japan Advanced Institute of Science and Technology, Nomi, Ishikawa, 923-1292, Japan. E-mail: t-hasobe@jaist.ac.jp, [b]PRESTO, Japan Science and Technology Agency (JST), 4-1-8 Honcho, Kawaguchi, Saitama, Japan. [c]Institute of Multidisciplinary Research for Advanced Materials, Tohoku University, Katahira, Sendai, 980-8577, Japan
†Electronic Supplementary Information (ESI) available: Experimental part, length-distributions, SEM images, XRD measurement, fluorescence lifetime, transient absorption spectroscopy. See DOI: 10.1039/b000000x/

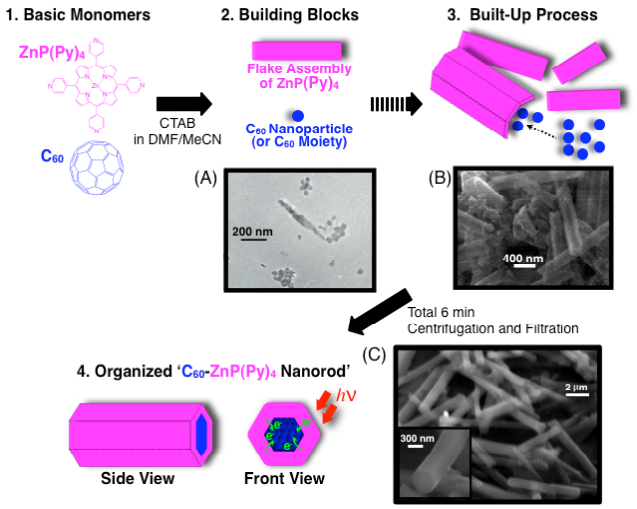

Fig. 1 Schematic illustration of organization process of C_{60} and $ZnP(Py)_4$ with CTAB in this study. CTAB is omitted for clarify. The electron micrographs show the time-dependent formations: (A) 1 min, (B) 3 min and (C) 6 min after injection.

A mixed proper ratio of $ZnP(Py)_4$ and C_{60} in DMF solution (*1.Basic monomers*) was injected into 7.5 times volume of continuously stirred 0.20 mM CTAB acetonitrile solution at room temperature. The final concentrations of $ZnP(Py)_4$ and C_{60} are 0.03 and 0.02 mM in DMF/acetonitrile (2/15, v/v), respectively. On injecting, they largely form $ZnP(Py)_4$ flake assemblies and C_{60}-based nanoparticles (ca. 5-20 nm in diameter), separately (*2.Building Blocks* & Fig. 1A).[7] With the diffusion of DMF into acetonitrile, the Zn-N axial coordination of pyridyl N-atoms to zinc atoms of $ZnP(Py)_4$ promotes the growth of aggregates, which continue to grow into a flake structure.[5c] In this case, the organization process of $ZnP(Py)_4$ moieties is derived from coordination bond in contrast with C_{60} assemblies based on relatively weak π-π interactions. Therefore, once injected, two different types of assemblies are quickly observed. Fig. 1B further shows the build-up formations of $ZnP(Py)_4$ and C_{60} after 3 min (*3.Built-Up Process*).[7] Then, after several minutes, C_{60}-$ZnP(Py)_4$ nanorods are finally formed (Fig. 1C). The reference $ZnP(Py)_4$ hexagonal nanotube without C_{60} was also prepared in the same manner for comparison [denoted as $ZnP(Py)_4$ nanotube]. It should be noted that the prepared samples were centrifuged at 14,000 rpm to remove CTAB by DMF/acetonitrile solvent repeatedly and filtrated to separate unbounded $ZnP(Py)_4$ and C_{60}. The self-assembled structures can be maintained for long hours. $ZnP(Py)_4$ nanotube shows a bar-like structure with a

large hollow hole [See ESI: Fig. S1A],[5c] whereas the hole is completely closed in C_{60}-ZnP(Py)$_4$ nanorods (Fig. 1C). C_{60}-ZnP(Py)$_4$ nanorods are analyzed as 4.12 ± 0.94 μm in length and 490 ± 90 nm in outside diameter by SEM images (Fig. S2).[8] As compared to ZnP(Py)$_4$ nanotubes analyzed as 2.13 ± 0.27 μm in length and 540 ± 30 nm in outside diameter (Fig. S2), a large increase of length direction from 2.13 to 4.12 μm relative to unchanged diameters (~500 nm) indicates that anisotropic crystal growth largely occurs toward the length direction due to π-π interaction of encapsulated C_{60} moieties within ZnP(Py)$_4$ assembly.[9-11]

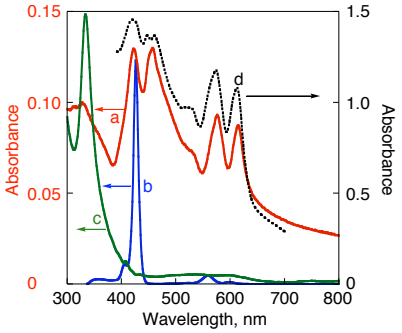

Fig. 2 Steady-state absorption spectra of (a) C_{60}-ZnP(Py)$_4$ nanorods in DMF/acetonitrile (2/15, v/v), (b) 1.3 μM ZnP(Py)$_4$ monomer in DMF, (c) 5 μM C_{60} monomer in DMF and (d) OTE/C_{60}-ZnP(Py)$_4$-nanorod film using an integrating sphere.

To examine electronic interaction in nanorod structures, we have measured steady-state absorption spectra of C_{60}-ZnP(Py)$_4$ nanorod in DMF/acetonitrile (2/15, v/v). In measurement of absorption spectra, we employed an integrating sphere to avoid scattering effect on the apparent absorption. The absorption spectrum of C_{60}-ZnP(Py)$_4$ nanorod exhibits much broader and more intense absorption in the visible and near infrared regions than those of the corresponding monomers: ZnP(Py)$_4$ or C_{60} in DMF (spectra *b* and *c*). Additionally, an absorption spectrum of C_{60}-ZnP(Py)$_4$ nanorod also becomes broader than that of ZnP(Py)$_4$ nanotube because of aggregated interactions of C_{60} assemblies or C_{60}-ZnP(Py)$_4$ interfaces (Fig. S4). Such a quite broad absorption property in the visible region is useful for solar energy conversion.

The singlet excited-state quenching of ZnP(Py)$_4$ by encapsulated C_{60} in C_{60}-ZnP(Py)$_4$ nanorods was investigated to obtain the overall fluorescence intensity quenching behavior with respect to the reference ZnP(Py)$_4$ nanotubes (Fig. 3). In steady-state fluorescence measurements, the fluorescence intensity of the porphyrin in C_{60}-ZnP(Py)$_4$ nanorod (trace *a*) is suppressed compared to that of the ZnP(Py)$_4$ nanotubes (spectrum *b*). This quenching is largely because of efficient PET from ^{1}ZnP(Py)$_4^*$ to C_{60} in nanorods.[4] Furthermore, additional quantitative electronic interplay on the photoexcited C_{60}-ZnP(Py)$_4$ nanorods could be evaluated by time resolved fluorescence spectroscopy. The insertion figure of Fig. 3 shows the fluorescence decay profiles of C_{60}-ZnP(Py)$_4$ nanorods, ZnP(Py)$_4$ nanotubes and ZnP(Py)$_4$ monomer, respectively. The fluorescence emission decay of C_{60}-ZnP(Py)$_4$ nanorods (trace *a*) was found to proceed faster than the ones observed on the ZnP(Py)$_4$ nanotubes (trace *b*) and monomer (trace *c*). By the biexponential fitting of the fluorescence decay of C_{60}-ZnP(Py)$_4$ nanorods, the fluorescence lifetimes (τ_f) were evaluated to be 180 ps (85%) and 1100 ps (15%), which are considerably shorter than those of ZnP(Py)$_4$ nanotubes [390 (65%) and 1870 (35%)] and ZnP(Py)$_4$ monomer [2200 ps (100%)]. It is reasonable to assume that photoinduced CS state [i.e. ZnP(Py)$_4^{\bullet+}$ and $C_{60}^{\bullet-}$] occurs in C_{60}-ZnP(Py)$_4$ nanorods. By comparing the τ_f of C_{60}-ZnP(Py)$_4$ nanorod with that of reference ZnP(Py)$_4$ nanotube, the CS rate-constant (k_{CS}) in C_{60}-ZnP(Py)$_4$ nanorods were calculated to be 3.0 x 10^9 s^{-1} (See: Fig. S5).

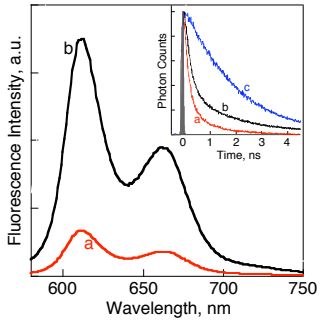

Fig. 3 Steady-state fluorescence spectra of (a) C_{60}-ZnP(Py)$_4$ nanorods and (b) ZnP(Py)$_4$ nanotubes in DMF/acetonitrile = 2/15, v/v. Inset: time-resolved fluorescence decays: (a) C_{60}-ZnP(Py)$_4$ nanorods, (b) ZnP(Py)$_4$ nanotubes and (c) 5 μM ZnP(Py)$_4$ monomer in DMF. λ_{ex} = 408 nm.

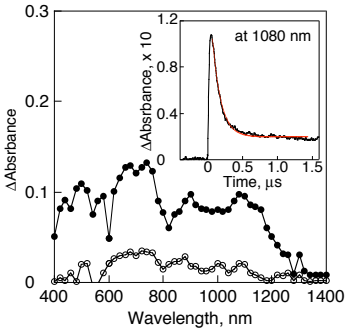

Fig. 4 Nanosecond transient absorption spectra of C_{60}-ZnP(Py)$_4$ nanorods in Ar-saturated DMF/acetonitrile (2/15, v/v) after the 532 nm laser irradiation at 0.1 μs (●) and 1.0 μs (○). Inset: the time profiles of $C_{60}^{\bullet-}$ monitored at 1080 nm.

Additional support for the above hypothesis comes from complementary transient absorption spectroscopy measurements performed after laser irradiation of C_{60}-ZnP(Py)$_4$ nanorods at 532 nm (Fig. 4). The characteristic features of the triplet-triplet absorption of ZnP(Py)$_4$ are missing in C_{60}-ZnP(Py)$_4$ nanorods, thus suggesting the efficient quenching of the singlet excited state by C_{60} moiety, which is sharp contrast with PET *via* ^{3}ZnP(Py)$_4^*$ in reference non-organized system: (C_{60}+ZnP(Py)$_4$)$_n$ (Fig. S5-7).[8,12] Interestingly, the transient spectra of C_{60}-ZnP(Py)$_4$ nanorods revealed transient bands corresponding to both $C_{60}^{\bullet-}$ at 1080 nm and ZnP$^{\bullet+}$ at 680 nm regions.[6d] Thus, considering all the above observations, it is reasonable to assume that the decay rates of the transient absorption bands can be attributed to charge recombination (CR), which occurs after the formation of a CS state in C_{60}-ZnP(Py)$_4$ nanorods. From the decay time profiles of these transient bands, the rate constants of the CR process are calculated to be 1.04 x 10^7 s^{-1} which corresponds to 100 ns for ZnP(Py)$_4^{\bullet+}$ and $C_{60}^{\bullet-}$.[13] The difference of PET pathways (i.e., via excited singlet or triplet state)[12] may have a great effect on light energy conversion properties (*vide infra*).

To evaluate solar energy conversion properties of C_{60}-ZnP(Py)$_4$ nanorods, we constructed a photoelectrochemical

This journal is © The Royal Society of Chemistry [year]

cell composed of C_{60}-ZnP(Py)$_4$ nanorod-modified SnO_2 optically transparent electrode (OTE) [denoted as OTE/C_{60}-ZnP(Py)$_4$-nanorod] by electrophoretic deposition (Fig. 5A).[4]

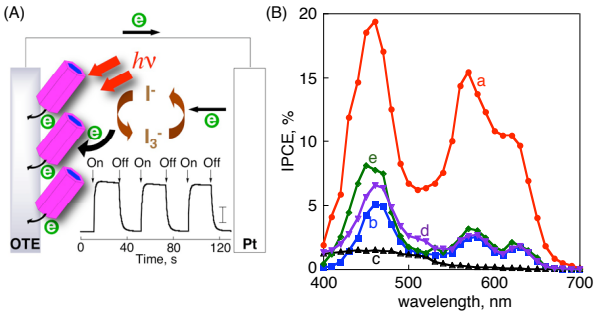

Fig. 5 (A) An Illustration of the photoelectrochemical solar cell. The insertion figure shows photocurrent generation responses under white light illumination (AM 1.5). Input Power: 82 mW cm^{-2}. The bar is 0.3 mA/cm^2. (B) Photocurrent action spectra of (a) OTE/C_{60}-ZnP(Py)$_4$-nanorod, (b) OTE/ZnP(Py)$_4$-nanotube, (c) OTE/C_{60}-assembly, (d) sum of spectra *b* and *c*, and (e) OTE/(ZnP(Py)$_4$+C_{60})$_n$; Electrolyte: 0.5 mol dm^{-3} LiI and 0.01 mol dm^{-3} I_2 in acetonitrile.

Fig. 2d shows an absorption spectrum of OTE/C_{60}-ZnP(Py)$_4$-nanorod on an OTE film after deposition, which largely agrees with that in solution. The photocurrent response recorded following the excitation of OTE electrodes shown in an insertion of Fig. 5A. The photocurrent response is prompt, steady and reproducible during repeated on/off cycles of the visible light illumination. Fig. 5B shows photocurrent action spectra of these composite films. The incident photon-to-photocurrent efficiency (IPCE)[4] spectrum of C_{60}-ZnP(Py)$_4$ film (spectrum *a*) shows a broad photoresponse in the visible region (maximum IPCE: ~20% at 460 nm), which parallels the corresponding absorption (spectrum *d* in Fig. 2). In particular, the maximum IPCE value of OTE/C_{60}-ZnP(Py)$_4$-nanorod (~20%: spectrum *a*) is much larger than the sum of two individual IPCE values (spectrum *d*: ~6.5%) of OTE/ZnP(Py)$_4$-nanotube (spectrum *b*) and OTE/C_{60}-assembly (spectrum *c*) under the same condition. Additionally, the maximum value of OTE/C_{60}-ZnP(Py)$_4$-nanorod (~20%) is also much larger than that of non-organized system: OTE/(ZnP(Py)$_4$+C_{60})$_n$ (spectrum e: ~8%).[8] These results clearly indicate that an organized structure between C_{60} and ZnP(Py)$_4$ as well as an excellent electron acceptor property of C_{60} has a great effect on the light energy conversion property. Such control of ultrafast PET pathway via ^{1}ZnP(Py)$_4^*$ in nanorod assembly largely contributes to the improvement of IPCE because of occurrence of strong fluorescence quenching in only ZnP(Py)$_4$ assembly (average quenching quantum yield: ~0.8 in Fig. S5). Photocurrent generation in the present system may be initiated by photoinduced CS from ^{1}ZnP(Py)$_4^*$ (^{1}ZnP*/ZnP$^{\bullet+}$ = –1.0 V vs NHE)[4c] to C_{60} (C_{60}/$C_{60}^{\bullet-}$ = –0.2 V vs NHE)[4b] in ZnP(Py)$_4$-C_{60} rather than direct electron injection to conduction band of SnO_2 (0 V vs NHE).[4b] The reduced C_{60} injects electrons into the SnO_2 nanocrystallites, whereas the oxidized porphyrin (ZnP/ZnP$^{\bullet+}$ = 1.0 V vs NHE)[4b] undergoes the ET reduction with the iodide ion (I_3^-/I^- = 0.5 V vs NHE).[4b]

In summary, we have successfully constructed new fullerene-encapsulated porphyrin hexagonal nanorods prepared in DMF/acetonitrile. These organized assemblies demonstrate controlled PET and efficient solar energy conversion properties. Such systems could pave for development of photoenergy conversion systems.

This work was partially supported by Grant–in–Aids for Scientific Research (No. 19710119 to T.H.) and special coordination funds for promoting science and technology from the Ministry of Education, Culture, Sports, Science and Technology, Japan.

Notes and references

1. (a) C. Joachim, J. K. Gimzewski and A. Aviram, *Nature*, 2000, **408**, 541; (b) G. M. Whitesides and B. Grzybowski, *Science*, 2002, **295**, 2418.
2. (a) R. vanHameren, A. M. vanBuul, M. A. Castriciano, V. Villari, N. Micali, P. Schon, S. Speller, L. MonsuScolaro, A. E. Rowan, J. A. A. W. Elemans and R. J. M. Nolte, *Nano Lett.*, 2008, **8**, 253; (b) K. Tashiro and T. Aida, *Chem. Soc. Rev.*, 2007, **36**, 189; (c) P. D. W. Boyd and C. A. Reed, *Acc. Chem. Res.*, 2005, **38**, 235; (d) C. M. Drain, G. Smeureanu, S. Patel, X. Gong, J. Garnod and J. Arijeloyea, *New J. Chem.*, 2006, **30**, 1834; (e) J. N. H. Reek, A. E. Rowan, M. J. Crossley and R. J. M. Nolte, *J. Org. Chem.*, 1999, **64**, 6653; (f) M. Wolffs, F. J. M. Hoeben, E. H. A. Beckers, A. P. H. J. Schenning and E. W. Meijer, *J. Am. Chem. Soc.*, 2005, **127**, 13484.
3. (a) D. Gust, T. A. Moore and A. L. Moore, *Acc. Chem. Res.*, 2001, **34**, 40; (b) D. Kim and A. Osuka, *J. Phys. Chem. A*, 2003, **107**, 8791.
4. (a) T. Hasobe, H. Imahori, P. V. Kamat, T. K. Ahn, S. K. Kim, D. Kim, A. Fujimoto, T. Hirakawa and S. Fukuzumi, *J. Am. Chem. Soc.*, 2005, **127**, 1216; (b) T. Hasobe, K. Saito, P. V. Kamat, V. Troiani, H. Qiu, N. Solladié, K. S. Kim, J. K. Park, D. Kim, F. D'Souza and S. Fukuzumi, *J. Mater. Chem.*, 2007, **17**, 4160.
5. (a) Z. Wang, C. J. Medforth and J. A. Shelnutt, *J. Am. Chem. Soc.*, 2004, **126**, 16720; (b) A. D. Schwab, D. E. Smith, B. Bond-Watts, D. E. Johnston, J. Hone, A. T. Johnson, J. C. dePaula and W. F. Smith, *Nano Lett.*, 2004, **4**, 1261; (c) J. S. Hu, Y. G. Guo, H. P. Liang, L. J. Wan and L. Jiang, *J. Am. Chem. Soc.*, 2005, **127**, 17090; (d) T. Kojima, T. Nakanishi, R. Harada, K. Ohkubo, S. Yamauchi and S. Fukuzumi, *Chem. Eur. J.*, 2007, **13**, 8714; (e) Q. Zhou, C. M. Li, J. Li, X. Cui, and D. Gervasio, *J. Phys. Chem. C*, 2007, **111**, 11216; (h) T. Hasobe, S. Fukuzumi and P. V. Kamat, *J. Am. Chem. Soc.*, 2005, **127**, 11884; (i) T. Hasobe, H. Oki, A. S. D. Sandanayaka and H. Murata, *Chem. Commun.*, 2008, 724.
6. (a) S. Fukuzumi and H. Imahori, in *Electron Transfer in Chemistry*, ed. V. Balzani, Wiley-VCH, Weinheim, 2001, vol. 2, pp. 927-975; (b) D. M. Guldi and M. Prato, *Acc. Chem. Res.*, 2000, **33**, 695; (c) M. U. Winters, E. Dahlstedt, H. E. Blades, C. J. Wilson, M. J. Frampton, H. L. Anderson and B. Albinsson, *J. Am. Chem. Soc.*, 2007, **129**, 4291; (d) F. D'Souza, P. M. Smith, M. E. Zandler, A. L. McCarty, M. Itou, Y. Araki and O. Ito, *J. Am. Chem. Soc.*, 2004, **126**, 7898.
7. We cannot exclude a possibility of composite molecular aggregation between ZnP(Py)$_4$ and C_{60} in Fig. 1A and B due to the strong interaction of porphyrins and C_{60} (See: ref. 2b and c). However, the definite discrimination is hard since these steps continuously proceed in solution.
8. In the case of preparation of ZnP(Py)$_4$ and C_{60} composite assemblies without CTAB [denoted as (ZnP(Py)$_4$+C_{60})$_n$], non-uniform rectangular structures are observed. See: Fig. S1B and C.
9. We have also measured XRD patterns of C_{60}-ZnP(Py)$_4$ nanorods and ZnP(Py)$_4$ nanotubes to examine the internal structures (Fig. S3). The pattern of C_{60}-ZnP(Py)$_4$ nanorod (pattern *a*) is approximately the same as that of ZnP(Py)$_4$ nanotube (pattern *b*). This suggests that ZnP(Py)$_4$ assemblies in the nanorods have quite similar structures to ZnP(Py)$_4$ nanotube, and C_{60} moieties are encapsulated within the ZnP(Py)$_4$ assemblies as shown in Fig. 1.
10. The crystal structure of ZnP(Py)$_4$ was previously reported. Considering the unit cell structure, growth direction of rod-assembly is *c* axis. See: Fig. S3, ref. 5c and H. Krupitsky, Z. Stein, I. Goldberg and C. E. Strouse, *J. Inclusion Phenom. Macrocyclic Chem.*, 1994, **18**, 177 and L. Kuan-Jiuh, *Angew. Chem., Int. Ed.*, 1999, **38**, 2730.
11. The final molar ratio between ZnP(Py)$_4$ and C_{60} was determined to be 3 : 1 by absorption measurement.
12. In contrast with C_{60}-ZnP(Py)$_4$ nanorod, PET via ^{3}ZnP(Py)$_4^*$ occurs in (ZnP(Py)$_4$+C_{60})$_n$. See: Fig. S5-7.
13. In an inset of Fig. 4, the minor and long lifetime species may be attributable to migration process of $C_{60}^{\bullet-}$ in encapsulated C_{60} assembly.

A graphical contents entry

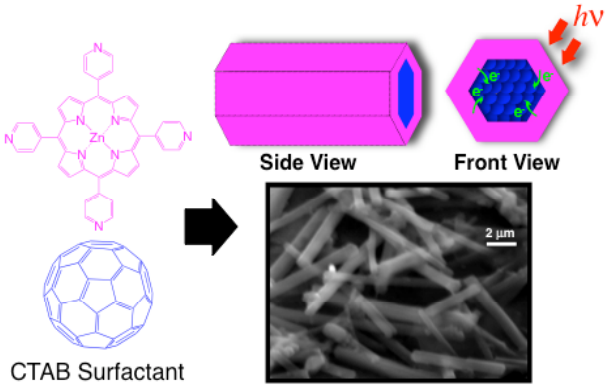

Fullerenes-encapsulated porphyrin hexagonal nanorods prepared in DMF/acetonitrile demonstrate efficient and characteristic photoinduced electron transfer and light energy conversion properties.

This journal is © The Royal Society of Chemistry [year]